49-L.0 MICROSTRUCTURE-STRENGTH RELATIONSHIPS OF HEAT-TREATED L-PBF TI-5AL-5V-5MO-3CR

Andrew Temple (ISU)
Faculty: Peter Collins (ISU)
Industrial Mentor:

This project initiated in Spring 2018 and was supported in part by Honeywell Federal Manufacturing & Technologies (FM&T), LLC. The research performed during this project will serve as the basis for a Ph.D. thesis program for Andrew Temple.

49-L.1 Project Overview and Industrial Relevance

Ti-5553 (Ti-5Al-5V-5Mo-3Cr, wt%) is a high-strength, metastable β titanium alloy commonly used in structural aircraft applications [49-L.1]. In general, β titanium alloys can be hardened to achieve much higher yield strengths than that of the more common α+β titanium alloy Ti-6Al-4V. Additionally, due to the lower β transus temperature resulting from the increased β stabilizer content, β alloys can be processed at lower temperatures [49-L-2]. Both the increased strength and lower processing temperature give the β alloys an advantage over the α+β alloys. There has also been increased research interest in recent years for producing β titanium alloy components via additive manufacturing.

Additive manufacturing (AM) is attractive in its ability to produce metastable beta titanium specimens that can retain a nearly 100% volume fraction β phase microstructure at room temperature [49-L.3]. With a metastable β microstructure in the as-built condition, heat treatments can be employed to achieve a wide range of microstructures and mechanical properties [49-L.4]. The obvious dependence of the mechanical properties on the underlying microstructure makes possible the systematic study of the microstructure-property relationships for the development and application of predictive equations to guide post-build processing of AM components. The application of a predictive equation, which is a function of microstructural measurements obtained from quantitative metallography, could enable materials engineers not only to predict the strength of as-built and heat-treated AM specimens, but also to predict the strength of "synthetic" specimens whose microstructure can be simulated using thermodynamic modeling. Such an equation is relevant for both alloy and process development.

49-L.2 Previous Work – Identifying potential strengthening mechanisms in beta titanium alloys

Previous work for this project has been focused on developing a microstructure-property database for heat-treated Ti-5553 additively manufactured by L-PBF. Twenty-seven samples were successfully heat-treated using the Gleeble 3800 Thermal-Mechanical Physical Simulation System, with a direct resistance heating system for precise control of heating/cooling rates and steady-state temperature holds during annealing and aging. A three-level full factorial design of experiments was followed during heat treatment, as shown in **Table 49-L.1**. A diagram of the heat-treatment scheme is shown in **Figure 49-L.1** as an example. The heat-treated specimens were tested in uniaxial tension at Westmoreland Mechanical Testing and Research, Inc. Following the uniaxial tensile tests, a transverse cross section was taken from the undeformed grip of each of the tensile specimens for metallographic preparation. Backscattered electron (BSE) micrographs were acquired with an FEI Teneo field emission scanning electron microscope (SEM) for quantitative microstructural analysis of the α phase fraction and the α-to-α inter-lath spacing using MIPAR Image Analysis Software.

The influence of inter-lath spacing on the yield strength of β titanium alloys is widely reported in the literature [49-L.5, 49-L.6, 49-L.7]. The governing strengthening mechanism is often reported to be the Hall-Petch relation which is expressed as follows [49-L.8, 49-L.9]:

$$\sigma_y = \sigma_0 + kD^{-1/2} \tag{49-L.1}$$

where σ_0 is the friction stress for starting dislocation movement in the matrix, k is the Hall-Petch coefficient for each material and D is the grain size. However, when applied to β titanium alloys, D is not taken to mean the β grain

size or the α lath thickness. Instead, D represents the mean free slip path, interparticle spacing, interphase spacing, etc. In this work, D is referred to as the α-to-α inter-lath spacing.

49-L.3 Recent Progress

49-L.3.1 Application of Hall-Petch and Solid Solution Strengthening

Dislocation motion is hindered by the large number of α/β interfaces in β titanium alloys, and as such, the strengthening due to the α phase can be explained by the Hall-Petch relation (**Figure 49-L.2**). It has been suggested that slip transfer across α/β interfaces is dependent on the alignment of incoming and outgoing slip systems [49-L.10]; however, much of this work has been done on α and α+β titanium alloys exhibiting only colony-type microstructures (i.e., a single α variant). More recent investigations into β titanium alloys have shown that the global Schmid factor dominates over geometrical factors, and α laths act to "filter out" anomalous (i.e., low Schmid factor) $\{110\}_{\beta}$ slip [49-L.11].

The value of the friction stress (833 MPa) for the line of best fit in **Figure 49-L.2** is in good agreement with the friction stress values reported by Jiang [49-L.7] (760-887 MPa) and Mantri [49-L.5] (830 MPa) for β titanium alloys. It is hypothesized that the friction stress of β titanium alloys is influenced by alloy composition, and thus, can be calculated based on solid solution strengthening theory.

49-L.3.2 Predicting Yield Strength

Equation 49-L.2 was used to make yield strength predictions as a function of only two measurable microstructural quantities: the α phase fraction and the α-to-α inter-lath spacing. A fixed nominal composition (5Al-5V-5Mo-3Cr-0.18O, wt%) was assumed for all specimens.

$$YS = F_V^{\alpha} \cdot (149 \cdot x_{Al}^{0.667} + 740 \cdot x_O^{0.667}) + F_V^{\beta} \cdot ((22 \cdot x_V^{0.7})^{0.5} + (247 \cdot x_{Cr}^{0.7})^{0.5})^2 + F_V^{\alpha} \cdot 210 \cdot d^{-1/2} \quad \text{(49-L.2)}$$

The resulting predictions were plotted against the experimentally measured yield strength values for each sample (**Figure 49-L.3**). The average error of the yield strength predictions was <3%, and the largest error was 8%. As with the previous equations developed for wrought and AM Ti-6Al-4V [49-L.12], solid solution strengthening was found to have the largest influence, contributing about 80% of the strengthening and setting the "base strength" for the alloy. The average solid solution strengthening contribution to the yield strength was 835 MPa, which is nearly identical to the value of the friction stress determined using the Hall-Petch relation. Strengthening beyond the "base strength" was attributed to the phase fraction and inter-lath spacing of the α phase, as governed by the Hall-Petch relation.

49-L.3.3 Virtual Experiments

As can be seen **Figure 49-L.4**, although the measured α phase fraction shows substantial variability from specimen-to-specimen, with no discernible trend in the raw data, the functional dependence of the yield strength on the α phase fraction is negligible (<50 MPa). In contrast, the inter-lath spacing shows a discernible trend, which appears to account for the vast majority of specimen-to-specimen yield strength variability.

49-L.4 Plans for Next Reporting Period

- Complete dissertation.
- Complete final oral examination.
- Graduate.
- Submit journal articles for publication.

49-L.5 References

[49-L.1] R. R. Boyer, R. D. Briggs, in Journal of Materials Engineering and Performance (2005), vol. 14, pp. 681–685.

[49-L.2] G. Lutjering, J. C. Williams, Titanium - 2nd Edition (Springer-Verlag, 2007).

[49-L.3] H. Schwab, F. Palm, U. Kühn, J. Eckert, Microstructure and mechanical properties of the near-beta titanium alloy Ti-5553 processed by selective laser melting. Materials and Design. 105, 75–80 (2016).

[49-L.4] H. D. Carlton, K. D. Klein, J. W. Elmer, Evolution of microstructure and mechanical properties of selective laser melted Ti-5Al-5V-5Mo-3Cr after heat treatments. Science and Technology of Welding and Joining. 24, 465–473 (2019).

[49-L.5] S. A. Mantri et al., Tuning the scale of α precipitates in β-titanium alloys for achieving high strength. Scripta Materialia. 154, 139–144 (2018).

[49-L.6] D. Sharma et al., The ageing response of direct laser deposited metastable β-Ti alloy, Ti–5Al–5Mo–5V–3Cr. Additive Manufacturing. 48 (2021), doi:10.1016/j.addma.2021.102384.

[49-L.7] B. Jiang, S. Emura, K. Tsuchiya, Microstructural evolution and its effect on the mechanical behavior of Ti-5Al-5Mo-5V-3Cr alloy during aging. Materials Science and Engineering A. 731, 239–248 (2018).

[49-L.8] E.O. Hall, Proc. Phys. Soc. Lond., B64 (1951), p. 747

[49-L.9] N.J. Petch, J. Iron Steel Inst., 174 (1953), p. 25

[49-L.10] M. F. Savage, J. Tatalovich, M. J. Mills, Anisotropy in the room-temperature deformation of α-β colonies in titanium alloys: Role of the α-β interface. Philosophical Magazine. 84, 1127–1154 (2004).

[49-L.11] C. Wang, M. A. Monclús, L. Yang, Y. Cui, M. T. Pérez-Prado, Effect of nanoscale α precipitation on slip activity in ultrastrong beta titanium alloys. Materials Letters. 264 (2020), doi:10.1016/j.matlet.2020.127398.

[49-L.12] B. J. Hayes et al., Predicting tensile properties of Ti-6Al-4V produced via directed energy deposition. Acta Materialia. 133, 120–133 (2017).

49-L.6 Figures and Tables

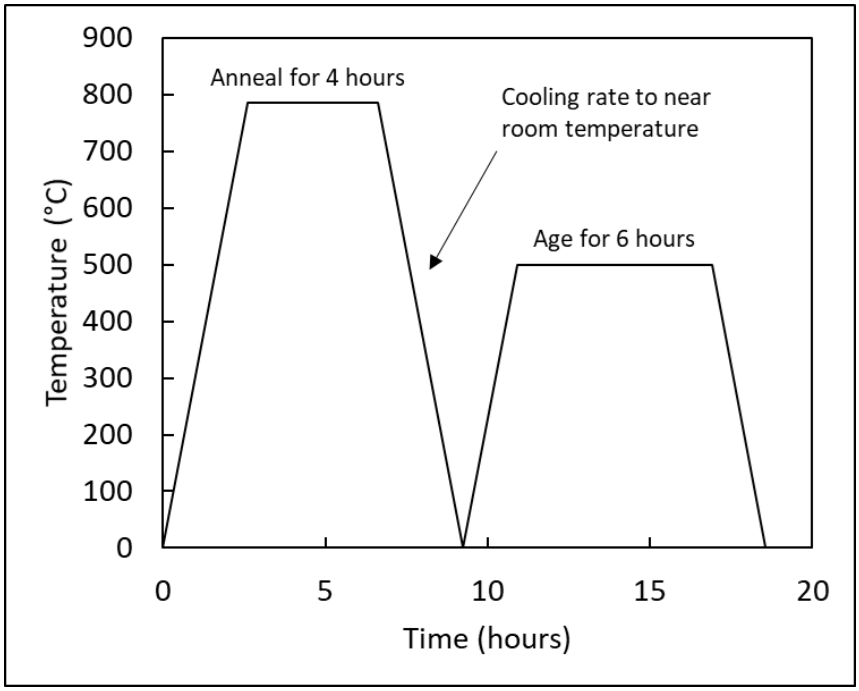

Figure 49-L.1. Example heat treatment schematic.

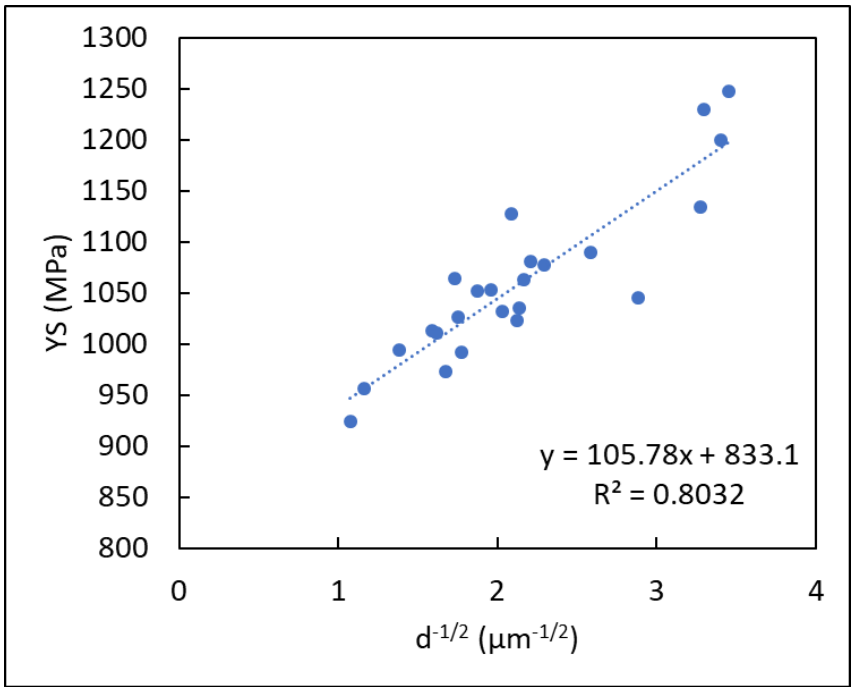

Figure 49-L.2. The relationship between the experimentally measured yield strength (YS) and the inverse of the square root of the inter-lath spacing ($d^{-1/2}$) for heat-treated L-PBF Ti-5553.

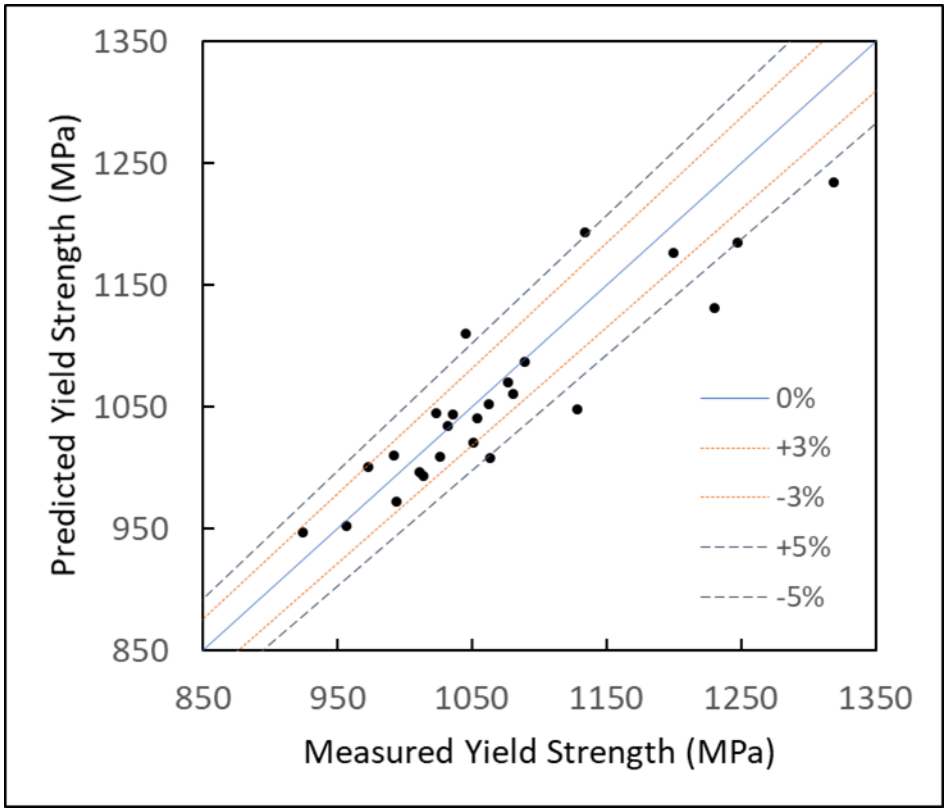

Figure 49-L.3. The predicted yield strength vs. the experimentally measured yield strength using **Equation 49-L.2**. All twenty-seven unique heat treatments can be represented by this single equation.

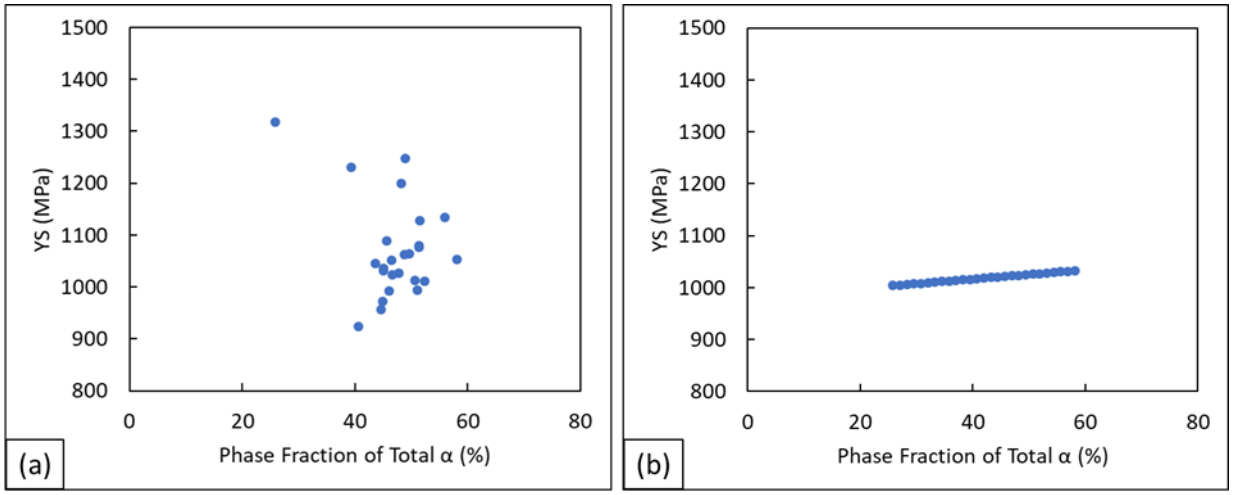

Figure 49-L.4. Scatter plot of YS vs. phase fraction of total α where (a) no observable trend can be established from the raw data and (b) the result from a virtual experiment illustrating the change in yield strength with the change in phase fraction assuming the inter-lath spacing is held constant at its mean value.

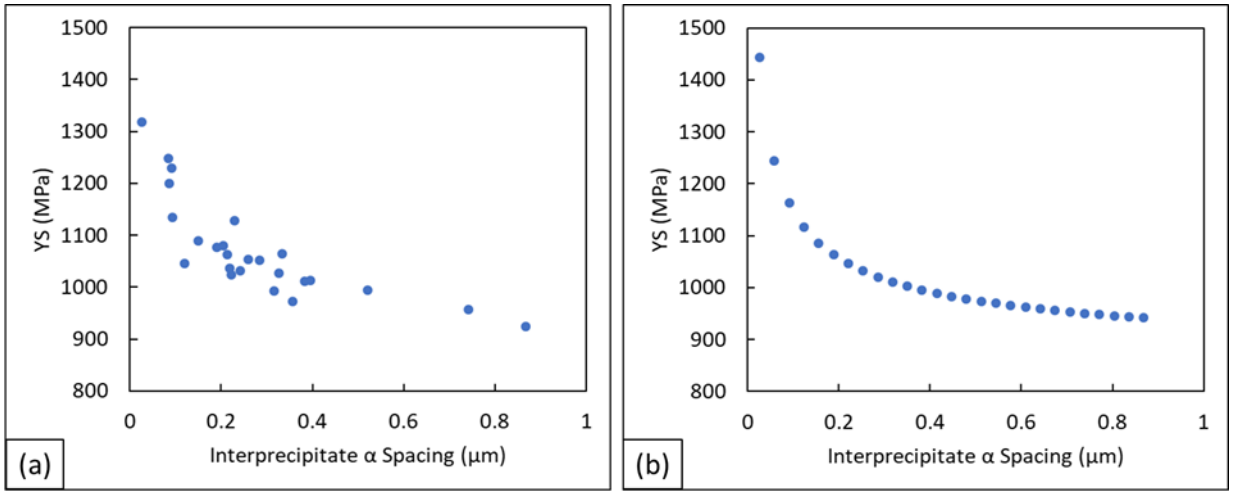

Figure 49-L.5. Scatter plot of YS vs. inter-lath spacing where (a) an observable trend can be established from the raw data and (b) the result from a virtual experiment illustrating the change in yield strength with the change in inter-lath spacing assuming the phase fraction is held constant at its mean value.

Table 49-L.1: Three-level full factorial design of experiments for heat treatments.

Variables	**Levels**		
	Low	**Mid**	**High**
Annealing temperature [°C]	700	745	785
Cooling rate [°C/min]	5	50	500
Aging temperature [°C]	500	575	650